

APPLICATION OF ENERGY DENSITY THEORY ON FINITE CRACKED BODIES

C. K. Chao* and R. C. Chang

ABSTRACT

A new concept of the energy release rate of a finite cracked body is proposed. Considering the global view of the strain energy density field, the new fracture parameter presented here is different from the conventional energy release rate that only depends on the stress field around the crack tip but neglects the influences induced by the boundary conditions on the far field. Based on the hypothesis of the energy density theory, fracture initiation and termination, respectively can be predicted by the local and global relative minima of the strain energy density function. The new energy release rate is then defined as the integration of the strain energy density along the fracture trajectory from the initiation point to the destination point. The results show that the difference between the new and the conventional energy release rate becomes more pronounced if the material has a large core region (or the material is more ductile) and if the height-width ratio of a finite cracked plate is comparatively small.

Key Words: energy release rate, crack, energy density theory.

I. INTRODUCTION

Energy release rate is one of the most important parameters in fracture mechanics. It has been successfully used to predict the maximum permissible applied load acting upon a cracked structure or the critical crack size within a component under fatigue or environmental influences. Griffith (1921) was the first to propose the idea that there is a driving force for crack extension resulting from the release of potential energy in the body with an inherent resistance to crack growth, associated with the necessity to supply surface energy for a newly formed crack surface. By using the existing mathematical development of Inglis (1913), Griffith formulated an energy balance approach, leading to a critical condition for fracture that could be written as an equality between the change in potential energy due to an increment of

crack growth and the resistance to this growth. Orowan (1948) and Irwin (1948) recognized that the most significant part of the release energy went, not into the surface, but was dissipated in the plastic flow around the crack tip and in the creation of a new plastic zone at the crack tips. Their modified energy balance approach to fracture is known as the Griffith-Orowan-Irwin theory. Based on this theory, the energy release rate is then established, which can be briefly stated as: the crack will grow if the release of the elastic energy is greater than the need of the surface energy during the creation of the new crack surface. However, it focuses on the local behavior of the crack tip and we will discuss the argument later.

On the other hand, the energy density theory (Sih and Chen, 1973; Sih, 1974) was proposed as a fracture criterion that provides an alternative approach to failure prediction. This theory possesses the inherent advantage of being able to treat all mixed mode crack extension problems. Unlike the conventional energy release rate and stress intensity factor that measure only the amplitude of the local stress, the energy density factor, the fundamental parameter in this theory, is defined as the coefficient of $1/r$ singular behavior of the volume strain energy density,

*Corresponding author. (ckchao@mail.ntust.edu.tw)

C. K. Chao is with the Department of Mechanical Engineering, National Taiwan University of Science and Technology, Taipei, Taiwan 106, R.O.C.

R. C. Chang is with the Department of Mechanical Engineering, St. John's and St. Mary's Institute of Technology, Taipei, Taiwan 251, R.O.C.

dw/dv , and is direction sensitive. The energy density theory has been widely used in the fracture communities and is found widely used in the literature (Gdoutos, 1984; Carpinteri, 1986; Shen and Nishioka, 2000; Zuo and Sih, 2000).

In this work, based on the energy density theory, a new concept of the energy release rate of a finite cracked body is discussed. The new parameter is defined as the integration of the strain energy density along the fracture trajectory that begins at the crack initiation and runs to the crack termination. In order to demonstrate the use of the present proposed parameter, numerical examples of zirconia and aluminum alloy are discussed in detail and shown in graphic form.

II. ELASTIC FIELD

In the plane elastic problem, the elastic field can be represented by two holomorphic functions $\Phi(z)$ and $\Psi(z)$ derived by Muskhelishvili (1953a), from which the stresses, resultant forces, and displacements are defined as

$$\begin{aligned}\sigma_{11} + \sigma_{22} &= 2[\Phi(z) + \overline{\Phi(z)}] \\ \sigma_{22} - i\sigma_{12} &= \Phi(z) + \overline{\Phi(z)} + z\overline{\Phi'(z)} + \overline{\Psi(z)} \\ X + iY &= -i[\phi(z) + z\overline{\Phi(z)} + \psi(z)]_{z_0}^z \\ 2\mu(u_1 + iu_2) &= \kappa\phi(z) - \psi(\overline{z}) - z\overline{\Phi(z)}\end{aligned}\quad (1)$$

where $z = x + iy$, $\Phi(z) = \phi'(z)$, $\Psi(z) = \psi'(z)$, and \overline{z} indicates the conjugate of z . The stress functions $\Phi(z)$ and $\Psi(z)$ defined in (1) can be determined by satisfying the boundary conditions. For the crack problem, Muskhelishvili (1953a) used the Hilbert problem method (1953b) to solve the mixed boundary value problem, where the boundary conditions on the crack surface are represented by a set of singular integral equations. Consider a finite plate having a central crack of length $2a$ with $2w$ in width and $2b$ in height subjected to a uniform stress σ_0 on the top and down boundaries, as shown in Fig. 1. The solution to this problem with no traction on the crack surface can be represented as a series form

$$\begin{aligned}\Phi(z) &= \frac{1}{\sqrt{z^2 - a^2}} \sum_{k=0}^m E_k z^k + \sum_{k=0}^m F_k z^k \\ \Psi(z) &= \frac{1}{\sqrt{z^2 - a^2}} \sum_{k=0}^m E_k z^k + \sum_{k=0}^m F_k z^k\end{aligned}\quad (2)$$

where E_k and F_k are complex constants, which can be determined to satisfy the outer boundary conditions on the remote boundaries. Because of the complexity, only an infinite cracked body has its analytical

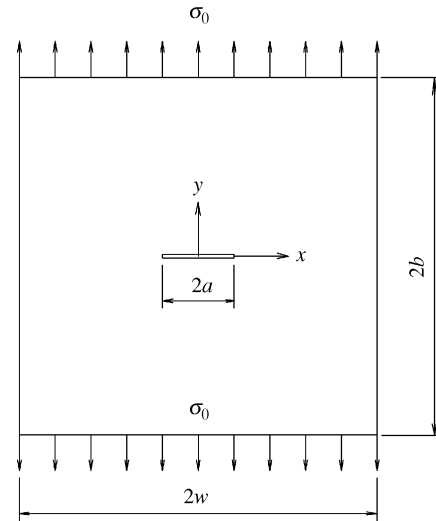


Fig. 1 The finite cracked body

solution, and all the discussions are restricted to the near-field region around the crack tip, where the effects of the outer boundary conditions are neglected. The discussion of the fracture phenomenon of the finite cracked body problem needs the help of numerical techniques. In this work, the complex constants E_k and F_k in (2) are determined to satisfy the boundary conditions at a discrete number of points. Based on the least square root method (Newman, 1971; Bowie and Freese, 1972), all the complex constants are solved to satisfy the uniform stress on the top and down surfaces as well as the traction-free condition on the left and right surfaces, with $m=96$ collocation points around the outer boundaries in equal space (Chao and Chang, 1991; Chao and Chang, 1992).

III. ENERGY RELEASE RATE

In general, energy balance and stress analysis are two fundamental methodologies to approach fracture phenomena. Based on Griffith's approach, a fracture parameter called energy release rate is defined as

$$G = \lim_{\Delta a \rightarrow 0} \frac{1}{\Delta a} \int_a^{a+\Delta a} \sigma_{2i}(r) u_i(r - \Delta a) dr \quad (3)$$

where a denotes the half crack length. The energy release rate can be regarded as the energy release of the elastic body for each crack growth length, while the crack begins to grow as the G value reaches the critical value G_c , an inherent material property.

On the other hand, the near-tip stress field can be expressed in terms of three kinds of stress intensity factors, K_I , K_{II} , K_{III} , which represent mode I (open mode), mode II (sliding mode), mode III (tearing mode) fracture patterns, respectively as (Irwin, 1957;

Sih *et al.*, 1962)

$$\begin{aligned}
\sigma_{11} &= \frac{K_I}{\sqrt{2\pi r}} \cos \frac{\theta}{2} (1 - \sin \frac{\theta}{2} \sin \frac{3\theta}{2}) \\
&\quad - \frac{K_{II}}{\sqrt{2\pi r}} \sin \frac{\theta}{2} (2 + \cos \frac{\theta}{2} \cos \frac{3\theta}{2}) \\
\sigma_{22} &= \frac{K_I}{\sqrt{2\pi r}} \cos \frac{\theta}{2} (1 + \sin \frac{\theta}{2} \sin \frac{3\theta}{2}) \\
&\quad + \frac{K_{II}}{\sqrt{2\pi r}} \sin \frac{\theta}{2} (\sin \frac{\theta}{2} \cos \frac{\theta}{2} \cos \frac{3\theta}{2}) \\
\sigma_{12} &= \frac{K_I}{\sqrt{2\pi r}} (\cos \frac{\theta}{2} \sin \frac{\theta}{2} \cos \frac{3\theta}{2}) \\
&\quad + \frac{K_{II}}{\sqrt{2\pi r}} \cos \frac{\theta}{2} (1 - \sin \frac{\theta}{2} \sin \frac{3\theta}{2}) \\
\sigma_{33} &= \frac{K_I}{\sqrt{2\pi r}} 2\nu \cos \frac{\theta}{2} - \frac{K_{II}}{\sqrt{2\pi r}} 2\nu \sin \frac{\theta}{2} \\
\sigma_{13} &= -\frac{K_{III}}{\sqrt{2\pi r}} \sin \frac{\theta}{2} \\
\sigma_{23} &= -\frac{K_{III}}{\sqrt{2\pi r}} \cos \frac{\theta}{2} \quad (4)
\end{aligned}$$

where r , θ denote the radius and angle of the polar coordinate at the crack tip, and the displacements are

$$\begin{aligned}
u_1 &= \frac{K_I}{2\mu} \sqrt{\frac{r}{2\pi}} \cos \frac{\theta}{2} (\kappa - 1 + 2\sin^2 \frac{\theta}{2}) \\
&\quad + \frac{K_{II}}{2\mu} \sqrt{\frac{r}{2\pi}} \sin \frac{\theta}{2} (\kappa + 1 + 2\cos^2 \frac{\theta}{2}) \\
u_2 &= \frac{K_I}{2\mu} \sqrt{\frac{r}{2\pi}} \sin \frac{\theta}{2} (\kappa + 1 - 2\cos^2 \frac{\theta}{2}) \\
&\quad - \frac{K_{II}}{2\mu} \sqrt{\frac{r}{2\pi}} \cos \frac{\theta}{2} (\kappa - 1 - 2\sin^2 \frac{\theta}{2}) \\
u_3 &= \frac{K_{III}}{\mu} \sqrt{\frac{r}{2\pi}} \sin \frac{\theta}{2} \quad (5)
\end{aligned}$$

where $\kappa=3-4\nu$ for plain strain and $\kappa=(3-\nu)/(1+\nu)$ for plain stress. The crack begins to grow when the stress intensity factor reaches the critical value K_{Ic} called fracture toughness which is a material property and independent of the loading type as well as the configuration of the cracked body. From (4), the strain energy density of a linear elastic body is given as

$$\frac{dw}{dv} = \frac{1}{\pi r} (a_{11}K_I^2 + 2a_{12}K_IK_{II} + a_{22}K_{II}^2 + a_{33}K_{III}^2) \quad (6)$$

where

$$\begin{aligned}
a_{11} &= \frac{(1+\nu)}{8E} [(3-4\nu-\cos\theta)(1+\cos\theta)] \\
a_{12} &= \frac{(1+\nu)}{8E} (2\sin\theta)[\cos\theta-(1-2\nu)] \\
a_{22} &= \frac{(1+\nu)}{8E} [4(1-\nu)(1-\cos\theta) \\
&\quad + (1+\cos\theta)(3\cos\theta-1)] \\
a_{33} &= \frac{(1+\nu)}{4E} \quad (7)
\end{aligned}$$

with E being the elastic modulus and ν the Poisson's ratio.

Since Griffith (1921) proposed the concept of energy release during crack growth, the energy release rate has become an important parameter in the study of fracture mechanics. The basic viewpoint of the energy release rate is that once the crack begins to grow, it never stops. That is, Griffith's energy release rate is based on the local viewpoint at the crack tip, but neglects global considerations affecting the crack growth.

The energy density theory is successfully proved in the application of mixed mode fracture behavior. It has been employed to predict crack trajectories, showing the results agreed well with experiments for plexiglass specimens that cracked suddenly with little or no detectable subcritical crack growth (Sih and Chen, 1973; Kipp and Sih, 1975). Assumed is that the crack would follow the path of minimum volume energy density, along which dilatation would dominate in contrast to distortion. For simplicity, the criterion will be stated in terms of dw/dv for a macrocrack. The energy density theory is based on the following hypotheses.

Hypothesis 1: Crack initiation is assumed to occur in the direction of the maximum or minimum dw/dv with reference to the space variables, say max. of $(dw/dv)_{\min}$.

Hypothesis 2: Crack initiation is assumed to take place when $(dw/dv)_{\min}$ reaches a critical characteristic value, say $(dw/dv)_c$.

Hypothesis 3: The onset of rapid crack propagation is assumed to start when the energy density S_{\min} associated with $(dw/dv)_{\min}$ also reaches a critical value, i.e., $S_{\min}=S_c$.

Then, the energy density factor S is defined as (Sih, 1974; Sih, 1991)

$$\frac{dw}{dv} = \frac{S}{r} \quad (8)$$

where S represents the intensity of the strain energy density. From (6) and (8), the energy density factor of a cracked body becomes

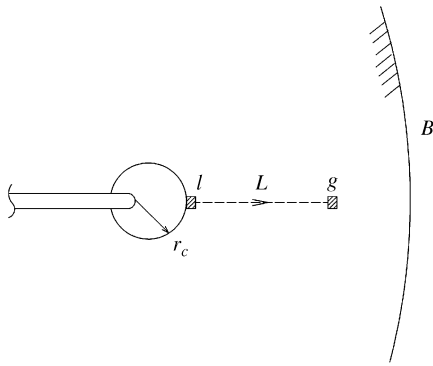


Fig. 2 Crack initiation, path, and termination

$$S = \frac{1}{\pi}(a_{11}K_I^2 + 2a_{12}K_I K_{II} + a_{22}K_{II}^2 + a_{33}K_{III}^2) \quad (9)$$

Eq. (9) shows S depends on the polar angle θ because the factors a_{11} , a_{12} , and a_{12} are dependent on θ . Moreover, considering the polar coordinate, since the volume is $rd\theta dr$ for unit thickness, S is still valid when r approaches 0. From (9), it follows:

$$S_c = \frac{(1+\nu)(1-2\nu)}{2\pi E} K_{Ic}^2 \quad (10)$$

where S_c is a material property. From (8), the critical value is defined as

$$\left(\frac{dw}{dv}\right)_c = \frac{S_c}{r_c} \quad (11)$$

where r_c is called the radius of a core region. It states that the crack begins to grow when the energy density factor S at the outside of the core region reaches S_c . The core region can be treated as the fundamental size connecting the microscopic material science and the macroscopic fracture mechanics. Continuum mechanics says the crack concerned has to be bigger than the core region. From (10) and (11), it follows:

$$r_c = \frac{(1+\nu)(1-2\nu)}{\pi} \left(\frac{K_{Ic}}{\sigma_u}\right)^2 \quad (12)$$

where σ_u denotes the ultimate stress of the uniaxial tension testing. The r_c value represents the character of the material, i.e., the material with the smaller (or larger) value of r_c tends to behave in a more brittle way (or more ductile).

Based on the strain energy density theory, we now propose to define a new energy release rate as

$$G_f = \int_{\ell}^g \left(\frac{dw}{dv}\right)_{\min}^{\max} dL \quad (13)$$

where $(dw/dv)_{\min}^{\max}$ indicates the max. of $(dw/dv)_{\min}$, ℓ is the local location of max. of $(dw/dv)_{\min}$ on the outer

core region, g is the global location of max. of $(dw/dv)_{\min}$, and L is the path of max. of $(dw/dv)_{\min}$, as shown in Fig. 2. The energy release rate G_f defined in (13) represents an explicit concept that integrates the strain energy density from the crack initiation, along the crack propagation, and to the crack termination. The energy density theory suggests that the fracture is due to the dilatational energy while the deformation is due to the distortional energy. The maximum dilatation energy occurs at the location of the minimum strain energy density, $(dw/dv)_{\min}$, while the maximum distortional energy occurs at the location of maximum strain energy density, $(dw/dv)_{\max}$. Once the crack begins to grow, the crack initiation occurs at the $(dw/dv)_{\min}$ on the border of the core region, i.e., at ℓ , so ℓ is the location of the crack initiation. The crack will propagate along the path of $(dw/dv)_{\min}$, denoted as L , and then grows to the global $(dw/dv)_{\min}$ point, denoted as g . The location of point g can be regarded as the terminal point of crack growth, at which the stress becomes compression. In general, the compressive stress resists crack growth. That is, once the crack begins to grow, it initiates at ℓ , propagates along the path L , and terminates at g . The distance between ℓ and g can be recognized as the tendency to crack growth. The system having the larger (or smaller) distance between ℓ and g tends to behave more unstably (or stably). For an infinite domain, the g point always prevails at infinity and the distance between ℓ and g becomes infinite, which presents the most unstable case.

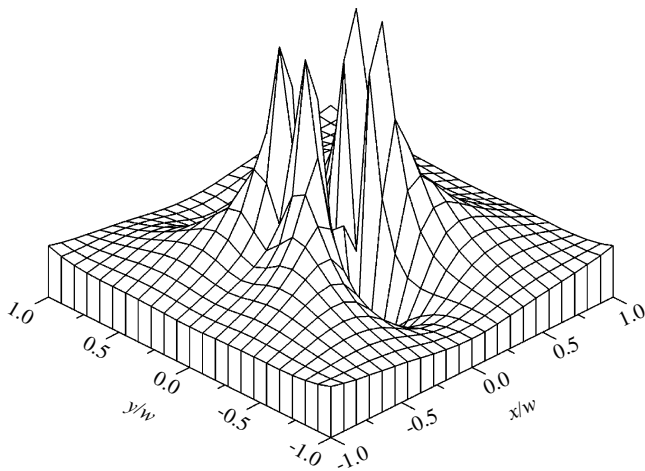
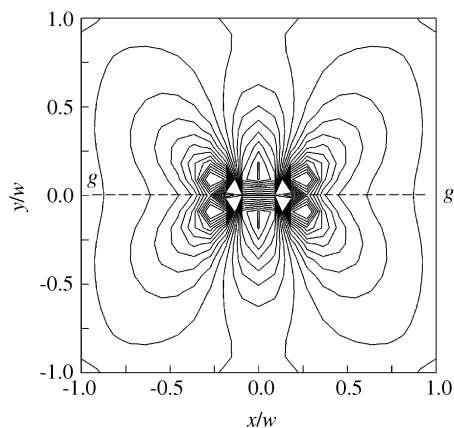
IV. NUMERICAL RESULTS AND DISCUSSIONS

Referring to Fig. 1, a finite cracked plate subjected to a uniform stress σ_0 is considered. The elastic solution can be obtained by formulating the Hilbert problem in conjunction with the boundary collocation method as discussed in Section II. Fig. 3 shows the distribution of the strain energy density with $b/w=1$, where the z axis represents the magnitude of dw/dv . It shows that the strain energy density attains its maximum value at the crack tip and then decays to its minimum value at the outer boundary. Fig. 4 shows the contours of the strain energy density of the entire finite plate, which illustrates that ℓ is located at the crack tip and g at the outer boundary, where the dashed line connecting the two points indicates the crack growth path. Figs. 5 and 6 illustrate the distribution and contours of the strain energy density for $b/w=0.3$. They show that, different from Figs. 3 and 4, the g point moves from the outer boundary into the inner domain.

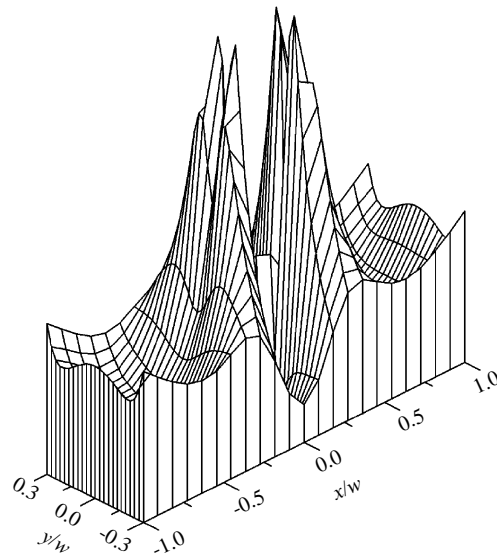
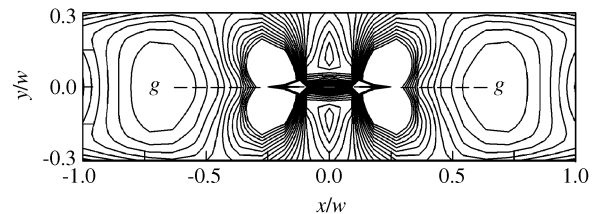
In this work, two materials are discussed, which are zirconia and aluminum alloy, of which the

Table 1 Fracture parameters of zirconia and aluminum alloy

	$\sigma_u(\times 10^6 \text{ Nm}^{-2})$	$K_{Ic}(\times 10^6 \text{ Nm}^{-3/2})$	$G_c(\times 10^3 \text{ Nm}^{-1})$	$r_c(\times 10^{-3} \text{ m})$	$S_c(\text{Nm}^{-1})$
Zirconia	700	10	0.47	0.043	52.9
Aluminum alloy	545	29.7	11.2	0.43	630

Fig. 3 Distribution of strain energy density with $b/w=1$ Fig. 4 Contours of strain energy density with $b/w=1$

fracture parameters are listed in Table 1. Figs. 7 and 8 show the difference between the conventional energy release rate G and the newly defined energy release rate G_f with various b/w ratios. For zirconia, Fig. 7 illustrates that the difference between the two parameters G and G_f gets larger for small b/w and gets closer as b/w increases. For aluminum alloy, Fig. 8 shows there is a certain gap between the two parameters and the difference between them gets larger as b/w decreases. Figs. 7 and 8 clearly show the obvious difference between G and G_f . It is seen that the difference between G and G_f of aluminum alloy is larger than that of zirconia, because the core region r_c of aluminum alloy is larger than that of zirconia,

Fig. 5 Distribution of strain energy density with $b/w=0.3$ Fig. 6 Contours of strain energy density with $b/w=0.3$

referring to Table 1. It means that aluminum alloy is more ductile than zirconia since its ℓ point is located farther from the crack tip. Moreover, the g point is located at the outer boundary when b/w is large, which means that rapid crack propagation prevails and the crack will grow immediately to the outer boundary. However, the difference between them becomes pronounced when b/w decreases, because the g point moves gradually into the inner domain. Therefore, the results show that the conventional energy release rate G is a limiting case of the newly defined energy release rate G_f where the ℓ is located at the crack tip, i.e., $r_c=0$, and g is located at the outer boundary. It also emphasizes that the newly defined energy release rate G_f provides a comprehensive fracture parameter in consideration of both the local and global viewpoints of the cracked body and modifies the lack of the conventionally defined parameter G that is restricted to brittle fractures and self-similar fracture behavior.

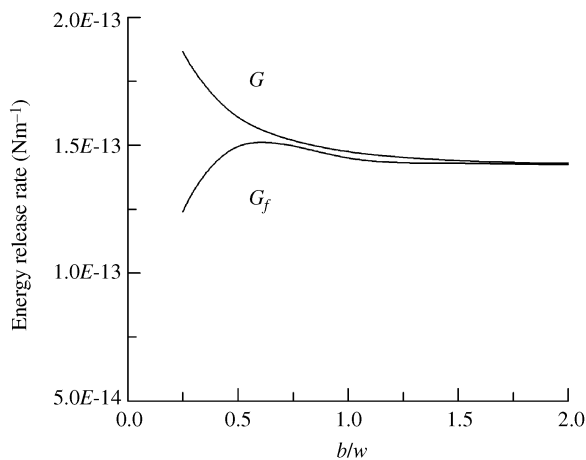


Fig. 7 Energy release rate of zirconia

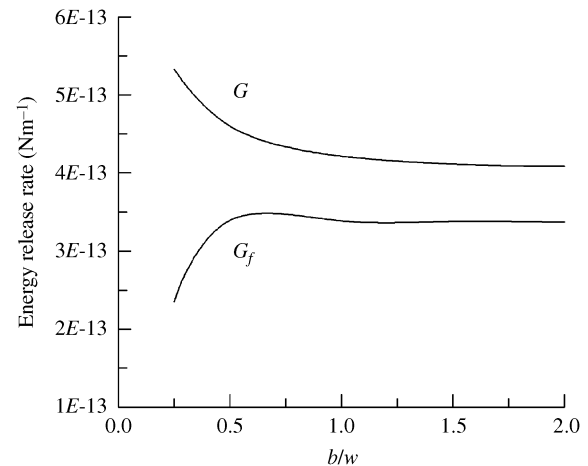


Fig. 8 Energy release rate of aluminum alloy

REFERENCES

- Bowie, O. L., and Freese, C. E., 1972, "Center Crack in Plane Orthotropic Rectangular Sheet," *International Journal of Fracture*, Vol. 8, pp. 49-58.
- Carpinteri, A., 1986, *Crack Growth and Material Damage in Concrete: Plastic Collapse and Brittle Fracture*, Engineering Application of Fracture Mechanics, Vol. 5, Martinus Nijhoff, Netherlands.
- Chao, C. K., and Chang, R. C., 1991, "Failure Analysis of a Thermoelastic Cracked Plate by Formulating the Hilbert Problem," *Journal of the Chinese Society of Mechanical Engineers*, Vol. 12, No. 2, pp. 128-136.
- Chao, C. K., and Chang, R. C., 1992, "Crack Trajectories Influenced by Mechanical and Thermal Disturbance in Anisotropic Material," *Theoretical and Applied Fracture Mechanics*, Vol. 17, No. 3, pp. 177-187.
- Inglis, C. E., 1913, "Stress in a Plate due to the Presence of Cracks and Sharp Corners," *Transactions of the Institute of Naval Architects*, Vol. 55, pp. 219-241.
- Gdoutos, E. E., 1984, *Problem of Mixed Mode Crack Propagation*, Engineering Application of Fracture Mechanics, Vol. II, Martinus Nijhoff, Netherlands.
- Griffith, A. A., 1921, "The Phenomena of Rupture and Flow in Solids," *Philosophical Transactions of the Royal Society of London*, A221, pp. 163-197.
- Irwin, G. R., 1948, *Fracture Dynamics, Fracturing of Metals*, American Society of Metals, pp. 147-166.
- Irwin, G. R., 1957, "Analysis of Stresses and Strains near the End of a Crack Transversing a Plate," *Journal of Applied Mechanics*, Vol. 24, pp. 361-364.
- Kipp, M. E., and Sih, G. C., 1975, "The Strain Energy Density Failure Criterion Applied to Notched Elastic Solids," *International Journal of Solids and Structures*, Vol. 11, No. 2, pp. 153-173.
- Muskhelishvili, N. I., 1953a, *Some Basic Problems of Mathematical Theory of Elasticity*, Noordhoff Pub., Groningen.
- Muskhelishvili, N. I., 1953b, *Singular Integral Equations*, Noordhoff Pub., Groningen.
- Newman, J. C., 1971, "An Improved Method of Collocation for the Stress Analysis of a Cracked Plate with Various Shaped Boundaries," *NASA TN-D-6376*.
- Orowan, E., 1948, *Fracture and Strength of Solids*, Reports of Progress in Physics, Vol. XII, p. 185.
- Shen, S., and Nishioka, T., 2000, "Fracture of Piezoelectric Materials: Energy Density Criterion," *Theoretical and Applied Fracture Mechanics*, Vol. 33, No. 1, pp. 57-65.
- Sih, G. C., Paris, P. C., and Erdogan, F., 1962, "Crack Tips, Stress-Intensity Factors for Plane Extension and Plate Bending Problems," *Journal of Applied Mechanics*, Vol. 29, pp. 306-312.
- Sih, G. C., and Chen, E. P., 1973, "Fracture Analysis of Unidirectional Composites," *Journal of Composite Materials*, Vol. 7, pp. 230-244.
- Sih, G. C., 1974, "Strain Energy Density Factor Applied to Mixed Mode Fracture," *International Journal of Fracture*, Vol. 10, No. 3, pp. 305-322.
- Sih, G. C., 1991, *Mechanics of Fracture Initiation and Propagation*, Kluwer Academic Publishers, The Netherlands.
- Zuo, J. Z., and Sih, G. C., 2000, "Energy Density Theory Formulation and Interpretation of Cracking Behavior for Piezoelectric Ceramics," *Theoretical and Applied Fracture Mechanics*, Vol. 34, No. 1, pp. 17-33.

*Manuscript Received: May 11, 2004
and Accepted: Jul, 02, 2004*